Finite-time fluctuation theorem for oscillatory lattices driven by a temperature gradient

Jinhong Li and Dahai He [*]

Department of Physics and Jiujiang Research Institute, Xiamen University, Xiamen 361005, China

The finite-time fluctuation theorem (FT) for the master functional, total entropy production, and medium entropy is studied in the one-dimensional Fermi-Pasta-Ulam-Tsingou-β (FPUT-β) chain coupled with two heat reservoirs at different temperatures. Through numerical simulations and theoretical analysis, we find that the nonequilibrium steady-state distribution of the one-dimensional FPUT-β chain violates the time-reversal symmetry. Thus, unlike the master functional, the total entropy production fails to satisfy the fluctuation relation for finite time. Meanwhile, we discuss the range of medium entropy production which obeys the conventional steady-state fluctuation theorem (SSFT) in the infinite time limit. Furthermore, we find that the generalized SSFT for medium entropy monotonically approaches the conventional SSFT as the time interval increases, irrespective of temperature difference, anharmonicity, and system size. Interestingly, the medium entropy production rate shows a nonmonotonic variation with anharomonicity, which comes from a competition mechanism of the phonon transport. Correspondingly, the difference between the generalized SSFT and the conventional SSFT shows similar nonmonotonic behaviors.

I. INTRODUCTION

Nonequilibrium statistical mechanics, unlike its equilibrium counterpart, lacks a unified theoretical framework. Therefore, it is not surprising that the fluctuation theorem has received significant attention since it quantifies the characteristics of the fluctuations of special physical quantity for a large class of systems, even when these systems are far from equilibrium. The fluctuation relation (FR) for entropy was first discovered in the numerical simulation of two-dimensional shear fluids [1,2], and proven by Gallavotti and Cohen based on a chaotic hypothesis [3]. The deterministic dynamics can be mapped onto a mixing Markov stochastic process when the chaotic hypothesis holds [4]; this result advances the derivation of the FR for stochastic dynamics. For a stochastic version of the FR, Kurchan [5] discussed the case of Langevin equation, which was later extended to general Markov processes in, e.g., stochastic lattice gas and Hamilton systems with random boundary conditions [6]. In early studies of FR for stochastic dynamics, FR holds only asymptotically under the long-time limit since the physical quantity considered is the entropy production of the medium Δs_t^m, which is called the conventional steady-state fluctuation theorem (SSFT) [7] of the following form:

$$\lim_{t \to +\infty} \frac{1}{\langle \Delta s_t^m \rangle} \ln \frac{P_t(s_t^m = p)}{P_t(s_t^m = -p)} = p. \qquad (1)$$

Here $s_t^m = \frac{\Delta s_t^m}{\langle \Delta s_t^m \rangle}$ is the dimensionless medium entropy production. The Crooks fluctuation theorem [8] reflects the relation between the probability density function (pdf) $P_F(s)$ of entropy production s for the forward process and the pdf $P_R(s)$

for the time-reversal process. Similar to the Jarzynski relation [9–12] it can be used to calculate the free energy difference between two equilibrium states, and the steady-state FR for total entropy production Δs_t^{tot}, which is the summation of the medium entropy production Δs_t^m and the system entropy production Δs_t [13], has been extensively studied [13–20]. Furthermore, a unification of FRs has been made, leading to the generalized SSFT [21]. Note that the master functional R_t (see Sec. II) is the same as Δs_t^{tot} in specified systems, such as the single-particle system. Thus, it can be seen that the steady-state FR on total entropy production, valid for arbitrary time interval, is given by

$$f_t(s) \equiv \frac{1}{\langle \Delta s_t^{\text{tot}} \rangle} \ln \frac{P_t(s_t^{\text{tot}} = s)}{P_t(s_t^{\text{tot}} = -s)} = s. \qquad (2)$$

Here $s_t^{\text{tot}} = \frac{\Delta s_t^{\text{tot}}}{\langle \Delta s_t^{\text{tot}} \rangle}$ is the dimensionless total entropy production.

Even for the long-time limit, the conventional SSFT in the form of Eq. (1) may break down for large fluctuations of certain physical quantities. For example, it has been shown that the conventional SSFT is satisfied only within the small fluctuation range of heat dissipation for a thermalized Brownian particle bounded in a moving potential [7,10]. The fluctuation of heat flow for a Brownian particle coupled to two thermal reservoirs at different temperatures has a similar result [22]. Furthermore, the distribution of large current fluctuation in the one-dimensional partially asymmetric zero-range process may violate the Gallavotti-Cohen symmetry [23]. For deterministic systems, the conventional SSFT for entropy production of a deterministic system connected with a isokinetic Gaussian thermostat is satisfied only for small fluctuations due to the singular boundary terms [24].

_____

[*]dhe@xmu.edu.cn

As for the one-dimensional chain with two ends respectively coupled to two stochastic heat baths at different temperatures, the cumulant generating function (CGF) [25–27] for heat flow from the left (right) bath into the harmonic chain satisfies the symmetry relation [28], which is further validated for anharmonic chains [29]. According to the large deviation theorem [30], if the CGF is differentiable everywhere, the large deviation function for the heat flow can be obtained by the Legendre transformation of the CGF, which also proves that the heat flow fluctuation satisfies the conventional SSFT for infinite time. Meanwhile, temporal asymmetries in the fluctuation-relaxation paths of a form of local heat flow have been found in the nonequilibrium FPUT-β model [31,32]. For the FPUT-β model coupled with the Nosé-Hoover thermostats, it has been numerically verified that the total heat flow conforms to the conventional SSFT [33]. The studies of the generalized exchange fluctuation theorem (GXFT) for the isolated near-integrable model show that the GXFT gives information on the ratio of probability of death to resurrection of solitons in the FPUT-α-β chain [34,35].

There are still some issues that require clarification: (a) the difference of total entropy production Δs_t^{tot} and master functional R_t, specifically, when one looks at a many-body interacting system in the nonequilibrium steady state driven by the temperature gradient, and (b) effects of the finite time interval on the deviation of the generalized SSFT from conventional SSFT. In this article, we study the fluctuations of several physical quantities for the FPUT-β system in the nonequilibrium steady state. We show that, first, Δs_t^{tot} is not odd time-reversed symmetrical, which is different from R_t. This leads to the violation of the FR for Δs_t^{tot} in the finite time interval. Second, we discuss the range of medium entropy production which obeys the conventional SSFT in the infinite time limit. Finally, we find that the generalized SSFT for Δs_t^m monotonically approaches the conventional SSFT irrespective of temperature difference, anharmonic strength, and system size, and its approaching speed is positively relevant with the rate of the medium entropy production. Interestingly, the rate of the medium entropy production varies with the anharmonic strength in a nonmonotonic way.

The rest of this paper is organized as follows. In Sec. II we introduce the FPUT-β model and the definition of entropies. In Sec. III we mathematically illustrate the time-reversal asymmetry of the nonequilibrium steady-state pdf and show that Δs_t^{tot}, which violates the steady-state FR for finite time, is different from R_t. Section IV discusses the range of Δs_t^m that obeys the conventional SSFT by looking at the decay property of the pdf. In Sec. V we study the time-dependent difference between the generalized SSFT for Δs_t^m and the conventional SSFT when temperature difference, anharmonic strength, and system size vary. A summary is provided in Sec. VI.

II. MODEL AND DEFINITION OF PHYSICAL QUANTITIES

We consider the FPUT-β chain of N particles with positions $\mathbf{x} = (x_1, x_2, \ldots, x_N)$ and velocities $\mathbf{v} = (v_1, v_2, \ldots, v_N)$. The particles are coupled to each other by nearest-neighbor FPUT-β potentials of the spring constant k and anharmonic strength β. The chain is connected to two Langevin heat baths at temperature T_L and T_R. The equations of motion are given

by

$$
\begin{aligned}
\dot{x}_i &= v_i, \\
\dot{v}_i &= -\frac{\partial U(\mathbf{x})}{\partial x_i} + (\delta_{i1} + \delta_{iN})[-\gamma_i v_i + g_i \xi_i(\tau)]
\end{aligned}
\tag{3}
$$

with

$$
\begin{aligned}
U(\mathbf{x}) = \sum_{i=1}^{N-1} &\left[\frac{k}{2}(x_i - x_{i-1})^2 + \frac{\beta}{4}(x_i - x_{i-1})^4 \right] \\
&+ \frac{k'}{2}\left(x_1^2 + x_N^2\right) + \frac{\beta'}{4}\left(x_1^4 + x_N^4\right),
\end{aligned}
\tag{4}
$$

where $\xi_i(\tau)$ is a Gaussian process with $\langle \xi_i(\tau) \rangle = 0$ and $\langle \xi_i(\tau)\xi_i(\tau') \rangle = 2\delta(\tau - \tau')$, γ_i is the viscosity of Gaussian noise, and g_i is the Gaussian strength with $g_i = \sqrt{\delta_{i1}\gamma_i T_L + \delta_{iN}\gamma_i T_R}$. Extra terms for the end particles with spring constant k' and anharmonic strength β' will allow us to specify different boundary conditions. In this paper, we used the fixed boundary condition by setting $k' = 1$ and $\beta' = 1$.

For a trajectory $X(\tau)$, the time-reversed dynamics, denoted by $X^\dagger(\tau)$, comes from the time-reversal mapping

$$
x_i^\dagger(\tau) = x_i(t - \tau), \quad v_i^\dagger(\tau) = -v_i(t - \tau)
\tag{5}
$$

with no changes at the form of potential function $U^\dagger(X^\dagger) = U(X^\dagger)$, the viscosity of Gaussian noise $\gamma_i^\dagger = \gamma_i$, and the Gaussian strength $g_i^\dagger = g_i$. The superscript symbol $\dagger$ represents the time-reversal mapping operation. The master functional R_t is given by the log-ratio of the path weights [13]

$$
\begin{aligned}
R_t &= \ln \frac{P[X(\tau)]_t}{P^\dagger[X^\dagger(\tau)]_t} \\
&= \ln \frac{P_0(X_0)}{P_0^\dagger(X_0^\dagger)} + \ln \frac{P[X(\tau) \mid X_0]_t}{P^\dagger[X^\dagger(\tau) \mid X_0^\dagger]_t} \\
&= R_t^0 + R_t^1,
\end{aligned}
\tag{6}
$$

which consists of a "boundary" term R_t^0, coming from the two pdfs for the initial states of the trajectories $X(\tau)$ and the time-reversed trajectories $X^\dagger(\tau)$, and a "bulk" term R_t^1 [13,21]. The subscript symbol t represents the time interval for the trajectories. In Eq. (6), P_0 and P_1 represent the pdf for the initial state and final state of the system, respectively. One can immediately find that $P_0^\dagger = P_1$. R_t^1 can easily be calculated in the path integral representation of the Langevin equation [6,8,13,36] as

$$
\begin{aligned}
R_t^1 &= \ln \frac{P[X(\tau) \mid X_0]_t}{P^\dagger[X^\dagger(\tau) \mid X_0^\dagger]_t} \\
&= -\int_0^t \frac{[-\gamma v_1(\tau) + g_1 \xi_1(\tau)]v_1(\tau)}{T_L} d\tau \\
&\quad - \int_0^t \frac{[-\gamma v_N(\tau) + g_N \xi_N(\tau)]v_N(\tau)}{T_R} d\tau \\
&= -\frac{q_L[X(\tau)]_t}{T_L} - \frac{q_R[X(\tau)]_t}{T_R} \\
&= \Delta s_t^m,
\end{aligned}
\tag{7}
$$

where q_L and q_R are the heat dissipation of the left bath and right bath, respectively. Equation (7) shows that the path weight of the forward trajectory is related to the backward

one in terms of the medium entropy production [37–40]. For any trajectory $X(\tau)$ of the original dynamic, we can find another particular realization of the noise ξ_i' produced by the same heat reservoir to obtain the corresponding time-reversed trajectory $X^\dagger(\tau)$ [41]. It means that any corresponding time-reversed trajectory $X^\dagger(\tau)$ is also the solution of Eq. (3), and then the original dynamic is microscopically reversible [8,42,43] thus leading to Eq. (7). It is worth noting that microscopic irreversibility would lead to the breakdown of well-known derivations of the fluctuation theorem, such as resetting stochastic dynamics [44,45]. The term "microscopically reversible" is distinct from the principle of detailed balance, which is equivalent to $R_t \equiv 0$ [8,36,46,47]. Therefore, the process we considered is microscopically reversible but violates detailed balance, and then we can get $R_t = R_t^0 + \Delta s_t^m$ when Δs_t^m is the entropy production of the medium for one trajectory $X(\tau)$. Moreover, the total entropy production for one trajectory $X(\tau)$ is

$$\Delta s_t^{\text{tot}} = \Delta s_t^m + \Delta s_t = R_t^1 + \Delta s_t, \qquad (8)$$

and $\Delta s_t = \ln \frac{P_0(X_0)}{P_1(X_t)}$ is a trajectory-dependent entropy production for the system [13].

It can be concluded from previous studies that the master functional obeys the FR for arbitrary time. Therefore, if the boundary term R_t^0 is equivalent to Δs_t, Δs_t^{tot} satisfies the FR for arbitrary time. Yet it is not generally the case, and as shown below, Δs_t^{tot} may fail to satisfy the steady-state FR for an interacting systems driven by the temperature gradient. Moreover, the medium entropy production Δs_t^m dissatisfies the steady-state FR in the finite time interval. In some special cases, the conventional SSFT with respect to Δs_t^m is only valid within a small fluctuation range.

III. DIFFERENCE BETWEEN R_t AND Δs_t

One can assume the functional $S_t^a[X(\tau)]$ of the original dynamics is odd symmetric after the time-reversal operation. It means that $S_t^{a\dagger}[X^\dagger(\tau)] = -S_t^a[X(\tau)]$ and $S_t^a[X(\tau)]$ satisfies a generalized FT in the form by

$$\frac{P(\{S_t^a = s^a\})}{P^\dagger(\{S_t^{a\dagger} = -s^a\})} = \langle \exp(R_t) | \{S_t^{a\dagger}\} = \{-s^a\} \rangle, \qquad (9)$$

which relates the pdf of the original process to the pdf of the time-reversed one and a conditional average [21]. According to the definition of the master functional R_t in Eq. (6), one has $R_t^\dagger[X(\tau)] = -R_t[X(\tau)]$. For the dimensionless quantity $r_t = \frac{R_t}{\langle R_t \rangle}$, Eq. (9) leads to a generalized FT given by

$$\frac{1}{\langle R_t \rangle} \ln \frac{P(r_t = r)}{P^\dagger(r_t^\dagger = -r)} = r. \qquad (10)$$

If the system is driven by the steady temperature difference rather than a time-dependent force, it will lead to $P^\dagger[X^\dagger(\tau) \mid X_0^\dagger]_t = P[X^\dagger(\tau) \mid X_0^\dagger]_t$. There is an equality $P_0(X) = P_1(X) = P_0^\dagger(X) = P_s(X)$ when the system is in the nonequilibrium steady state. Thus one finds

$$P^\dagger(S_t^a = -s^a) = P(S_t^a = -s^a). \qquad (11)$$

Moreover, due to $r_t^\dagger[X(\tau)] = r_t[X(\tau)]$ the equality (11) can be rewritten for $S_t^a = r_t$ as

$$P^\dagger(r_t^\dagger = -r) = P(r_t = -r). \qquad (12)$$

Substituting Eq. (12) into Eq. (10) leads to the finite-time FR for R_t in the form as

$$f_t(r) \equiv \frac{1}{\langle R_t \rangle} \ln \frac{P(r_t = r)}{P(r_t = -r)} = r, \qquad (13)$$

where $f_t(r)$ is defined as the scaled logarithmic ratio. The system entropy production Δs_t is different from the boundary term R_t^0 when $P_0^\dagger(X_0^\dagger) = P_1(X_0^\dagger) \neq P_1(X_t)$ [48], and it means that the total entropy production Δs_t^{tot}, unlike R_t, may not satisfy the odd time-reversed symmetry ($\Delta s_t^\dagger[X^\dagger(\tau)] = -\Delta s_t[X(\tau)]$) and the finite-time FR in the form of Eq. (13). It should be noted that in previous studies [9,13–15,18,21], e.g., for the overdamped motion of a colloidal particle or the nonequilibrium process of a system from one equilibrium state to another, the distribution function of the final state $P_1(X)$ satisfies $P_1(X) = P_0^\dagger(X^\dagger)$. It means that R_t is equivalent to Δs_t^{tot} for arbitrary time and $\Delta s_t^{\text{tot}}[X(\tau)]$ is odd symmetric after the time-reversed operation in those cases. However, it is not generally valid.

Here we show that the nonequilibrium steady-state distribution of the many-body system violates the time-reversed symmetry, namely, $P_s(X) \neq P_s(X^\dagger)$. The Fokker-Planck equation [36,49] corresponding to the forward process is given by

$$\frac{\partial P(X, \tau)}{\partial \tau} = -\sum_{i=1}^{N} \left\{ \frac{\partial}{\partial x_i} v_i + \frac{\partial}{\partial v_i} \left[-\frac{\partial U(\mathbf{x})}{\partial x_i} \right. \right. \\ \left. \left. -\gamma v_i + D_i \frac{\partial}{\partial v_i} \right] \right\} P(X, \tau), \qquad (14)$$

where $D_i = g_i^2 = \delta_{i1}\gamma_i T_L + \delta_{iN}\gamma_i T_R$, and the time-reversal Fokker-Planck equation is written by

$$\frac{\partial P^\dagger(X^\dagger, \tau')}{\partial \tau'} = -\frac{\partial P(X^\dagger, \tau)}{\partial \tau} \\ = -\sum_{i=1}^{N} \left\{ \frac{\partial}{\partial x_i} v_i + \frac{\partial}{\partial v_i} \left[-\frac{\partial U(\mathbf{x})}{\partial x_i} \right. \right. \\ \left. \left. +\gamma v_i - D_i \frac{\partial}{\partial v_i} \right] \right\} P(X^\dagger, \tau) \qquad (15)$$

with $\tau' = t - \tau$. Similar to $P_0^\dagger = P_1$, we can get $P^\dagger(X^\dagger, \tau') = P(X^\dagger, \tau)$. When the system is in the nonequilibrium steady state, one has

$$\frac{\partial P(X, \tau)}{\partial \tau} = \frac{\partial P^\dagger(X^\dagger, \tau')}{\partial \tau'} = 0, \qquad (16)$$

and $P(X, \tau) = P_s(X)$. Here one can use a simple proof by contradiction. If $P_s(X) = P_s(X^\dagger)$, one can find from
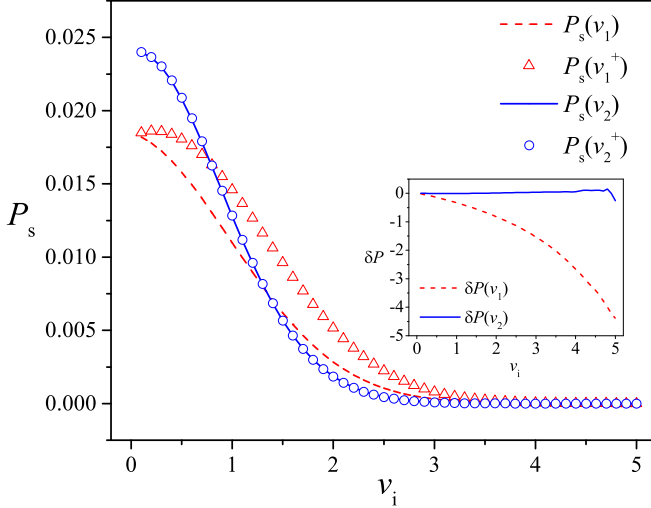
FIG. 1. Comparing the nonequilibrium steady-state pdf $P_s(X)$ with the time-reversed pdf $P_s(X^\dagger)$. Here we plot the dimensionality-reduction distribution with respect to the velocity $v_{1,2}$ for the FPUT-β model of $N = 2$. Inset: Relative difference $\delta P \equiv \frac{P_s(X) - P_s(X^\dagger)}{P_s(X)}$. The dashed and solid lines represent $P_s(v_1)$ and $P_s(v_2)$, respectively. The triangle and circle symbols represent $P_s(v_1^\dagger)$ and $P_s(v_2^\dagger)$, respectively. In the simulations, we set $k = 1$ and $\beta = 1$. The temperatures of heat baths are set by $T_L = 1.5$ and $T_R = 0.5$ and the viscosity $\gamma = 1$.

Eqs. (14)–(16) that

$$-\sum_{i=1}^{N} \frac{\partial}{\partial v_i} \left(-\gamma v_i + D_i \frac{\partial}{\partial v_i} \right) P_s(X)$$
$$= \sum_{i=1}^{N} \frac{\partial}{\partial v_i} \left(-\gamma v_i + D_i \frac{\partial}{\partial v_i} \right) P_s(X^\dagger) = 0 \quad (17)$$

and

$$-\sum_{i=1}^{N} \left[\frac{\partial}{\partial x_i} v_i + \frac{\partial}{\partial v_i} \left(-\frac{\partial U(\mathbf{x})}{\partial x_i} \right) \right] P_s(X) = 0. \quad (18)$$

$P_s(X)$ satisfies both Eq. (17) and Eq. (18). Since $D_1 \neq D_N$, Eq. (17) does not have permutation symmetry with respect to v_1 and v_N, indicating that in addition to the trivial solution $P_s(X) = 0$, the solution $P_s(X)$ of Eq. (17) also does not have permutation symmetry with respect to v_1 and v_N. However, the solution $P_s(X)$ of Eq. (18) have permutation symmetry with respect to v_1 and v_N. The contradiction indicates that the nonequilibrium steady-state distribution of the system does not satisfy the time-reversal symmetry, i.e., the above assumption $P_s(X) = P_s(X^\dagger)$ is invalid. Note that for the case of one particle coupled to two thermal reservoirs at different temperatures, the system is effectively in the equilibrium state, and the steady-state distribution of the system $P_s(X)$ satisfies the time-reversal symmetry [$P_s(X) = P_s(X^\dagger)$].

Since the time complexity to calculate $P_s(X)$ numerically for the FPUT-β system increases exponentially with N, we perform numerical simulations for the FPUT-β system with $N = 2$ in order to verify $P_s(X) \neq P_s(X^\dagger)$. In Fig. 1, for the sake of visualization, the dimensionality-reduction distributions with respect to the velocity v_1 or v_2 are plotted. For
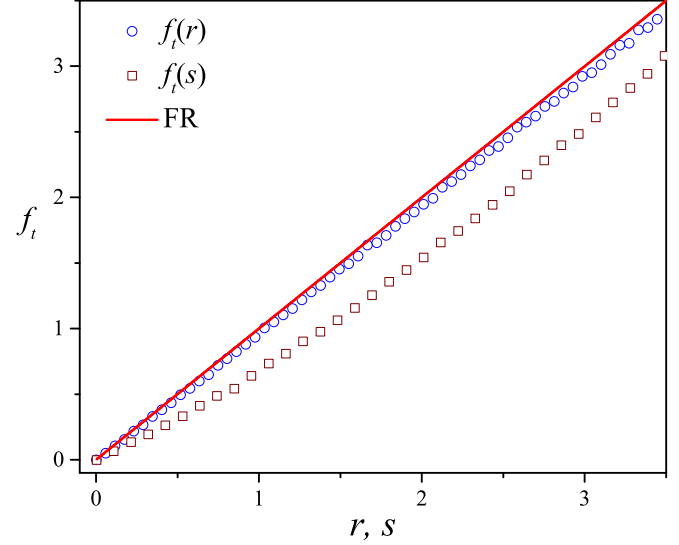
FIG. 2. Comparing the scaled logarithmic ratio $f_t(r)$ and $f_t(s)$ with the FR when the time interval $t = 1$. The FR is represented by the solid line with a slope of 1. The parameters are the same as those for Fig. 1.

example, a reduced pdf $P_s(v_1)$ is plotted for an intersecting surface of the phase space, for which $x_1 = x_2 = 0$, $v_2 = 0$. One can find $P_s(X) \neq P_s(X^\dagger)$ from Fig. 1. When the time interval is nonzero ($t \neq 0$), any combination of the initial state and the final state will appear with a nonzero probability. We consider the subset of initial state $\widetilde{X}_0 \in \{X_0 \mid x_1 = x_2 = 0, v_1 = 0\}$ and the subset of final state $\widetilde{X}_t \in \{X_t \mid x_1 = x_2 = 0, v_2 = 0\}$. According to Fig. 1, it is obvious that $P_0(\widetilde{X}_0) = P_s(\widetilde{X}_0) = P_s(\widetilde{X}_t^\dagger) = P_t^\dagger(\widetilde{X}_t^\dagger)$ and $P_t(\widetilde{X}_t) = P_s(\widetilde{X}_t) \neq P_s(\widetilde{X}_0^\dagger) = P_0^\dagger(\widetilde{X}_0^\dagger)$, which means $\Delta s_t^\dagger[X^\dagger(\tau)] \neq -\Delta s_t[X(\tau)]$. Then the pdf $P(\Delta s_t^{\text{tot}})$ for the total entropy production may not satisfy Eq. (9) with $S_t^a = \Delta s_t^{\text{tot}}$ and thus dissatisfy the finite-time FR in the form of Eq. (13). For verification, we numerically calculate the scaled logarithmic ratio $f_t(r)$ and $f_t(s) \equiv \frac{1}{\langle \Delta s_t^{\text{tot}} \rangle} \ln \frac{P(s_t^{\text{tot}} = s)}{P(s_t^{\text{tot}} = -s)}$ with the dimensionless quantity $s_t^{\text{tot}} = \frac{\Delta s_t^{\text{tot}}}{\langle \Delta s_t^{\text{tot}} \rangle}$.

Indeed, it can be found from Fig. 2 that $f_t(s) \neq s$ fails to obey the FR in the finite time interval $t = 1$, which is different from $f_t(r) = r$.

IV. RANGE OF Δs_t^m OBEYING THE CONVENTIONAL SSFT

According to the definition of Δs_t^m [Eq. (7)], one can find that Δs_t^m satisfies the odd time-reversed symmetry ($\Delta s_t^{m\dagger}[X^\dagger(\tau)] = -\Delta s_t^m[X(\tau)]$). The generalized SSFT [21] about Δs_t^m for arbitrary time interval t is obtained from Eq. (9) as

$$f_t(p) \equiv \frac{1}{\langle \Delta s_t^m \rangle} \ln \frac{P(s_t^m = p)}{P(s_t^m = -p)}$$
$$= p + \frac{1}{\langle \Delta s_t^m \rangle} \ln \langle e^{R_t^0} | s_t^m = p \rangle, \quad (19)$$

where we replace the functional S_t^a by the dimensionless quantity s_t^m. It can be seen from Eq. (19) that, due to the existence

of the boundary term R_t^0, the form of the generalized SSFT for Δs_t^m is affected by the second term in the second line of Eq. (19), which is determined by p and the time interval t.

The CGF $g(\lambda)$ is given in the form

$$g(\lambda) = \lim_{t \to +\infty} \frac{1}{t} \ln \langle e^{\lambda \Delta s_t^m} \rangle. \qquad (20)$$

Whether the system is a simple harmonic chain or a nonharmonic chain, the CGF has the following symmetry [28,29]:

$$g(\lambda) = g(1 - \lambda). \qquad (21)$$

If $g(\lambda)$ exists and is differentiable for all $\lambda \in R$, the Gartner-Ellis Theorem states that s_t^m satisfies a large deviation principle [30],

$$\lim_{t \to +\infty} P(s_t^m = p) \sim e^{-tI(p)}, \qquad (22)$$

with the large deviation function $I(p)$ given by the Legendre transform of $e(\lambda)$

$$I(p) = \lambda^* p - g(\lambda^*), \qquad (23)$$

where λ^* is given by $\frac{dg(\lambda)}{d\lambda}|_{\lambda = \lambda^*} = p$. Equation (21) and Eq. (23) mean that $I(p)$ also has the following symmetry:

$$I(p) - I(-p) = p, \qquad (24)$$

which is also equivalent to the infinite-time conventional SSFT for Δs_t^m in the form

$$\lim_{t \to +\infty} f_t(p) = p. \qquad (25)$$

Equation (19) and Eq. (25) are not contradictory since Eq. (25) requires that

$$\lim_{t \to +\infty} \frac{1}{\langle \Delta s_t^m \rangle} \ln \langle e^{R_t^0} | s_t^m = p \rangle \to 0. \qquad (26)$$

However, this is a conclusion based on Eq. (23), which requires $e(\lambda)$ to exist and be differentiable everywhere. For the example in Ref. [7], Eq. (24) is satisfied only when $p < 1$, which means that the infinite-time conventional SSFT for Δs_t^m (25) also holds only when $p < 1$, because the singularity of $e(\lambda)$ destroys the derivability of $e(\lambda)$. This is called the extension of FT, and similar results can be also found in Refs. [22] and [24]. For our system, the property of $e(\lambda)$ is difficult to obtain, which will prevent us from strictly determining the range of p that satisfies the conventional SSFT for infinite time. To investigate this, we numerically calculate $f_t(p)$ as t increases.

It can be found from Fig. 3 that when t is small, $f_t(p) \neq p$, which is consistent with the prediction of Eq. (19). However, as t increases, $f_t(p) \to p$, which is consistent with Eq. (25). Since it is extremely difficult to calculate $f_t(p)$ when p is very large, the behavior of $f_t(p)$ that changes with the increasing t can be studied only for a limited p. The infinite-time conventional SSFT may not be valid for the larger p, but the results in Fig. 3 show that the conventional SSFT is valid for large t when $p \in [0, p^*]$. It is difficult to determine the effective boundary p^* for the infinite-time conventional SSFT regardless of the use of numerical simulation calculation or analytical methods. However, similar to the analysis in [7] and [4], from the analysis of the pdf for boundary term R_t^0
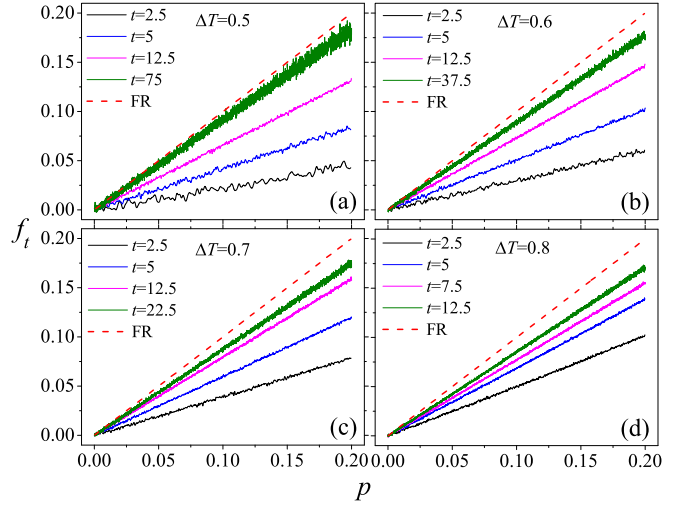
FIG. 3. Comparing the scaled logarithmic ratio $f_t(p)$ for different time intervals t with FR for (a) $\Delta T = 0.5$, (b) $\Delta T = 0.6$, (c) $\Delta T = 0.7$, and (d) $\Delta T = 0.8$. The dashed curve is a straight line with a slope of 1 that represents FR for the medium entropy production Δs_t^m. The temperature difference $\Delta T = \frac{1}{2T}(T_L - T_R)$ and average temperature $T = \frac{1}{2}(T_L + T_R) = 1$. The other parameters are the same as those for Fig. 1.

and bulk term Δs_t^m, we can make some qualitative discussion about whether the boundary p^* is a finite value.

It is shown in Fig. 4 that the pdf for $\Delta s_t^m = R_t - R_t^0$ is dominated by the contribution from the boundary term R_t^0 when t is small. As t increases, the probability distribution for R_t^0 tends to be a stable distribution because R_t^0 is not a cumulative amount of time and related to only the initial and final states of the system. We also found that even though for the large values the pdf for Δs_t^m and R_t tend to coincide, this means that p^* may be infinite. It should be noted that the value range of Δs_t^m and R_t in Fig. 4 is limited, yet so far it is inconclusive whether the distributions still coincide when Δs_t^m and R_t tend to infinity. However, in terms of our numerical results, one may make a reasonable assumption that the stable distribution of R_t^0 still has exponential tails for the large values. If so, these exponential tails will dominate the pdf for Δs_t^m at very large values since the pdf for R_t is concave.
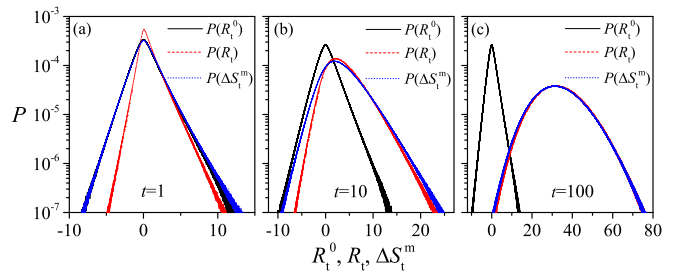
FIG. 4. The nonequilibrium steady-state pdf P as a function of the boundary term R_t^0, master functional R_t, and medium entropy production Δs_t^m for (a) $t = 1$, (b) $t = 10$, and (c) $t = 100$. The solid, dashed, and dotted lines correspond to the steady-state pdf $P(R_t^0)$, $P(R_t)$, and $P(\Delta s_t^m)$, respectively. The parameters are the same as those for Fig. 1.
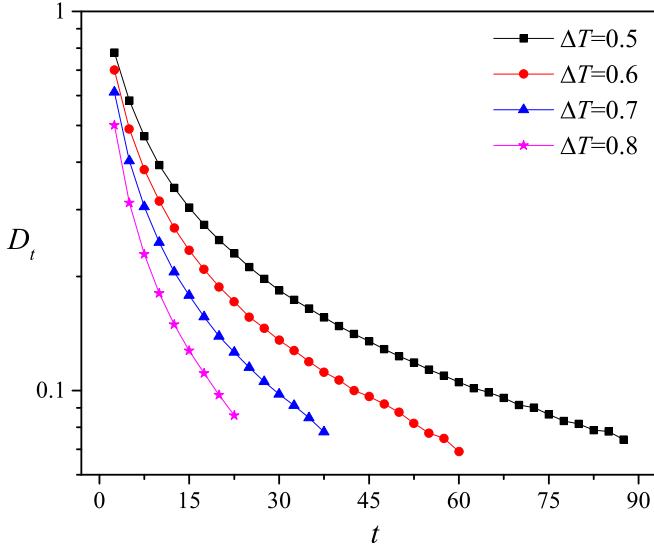
FIG. 5. D_t as a function of time interval t for temperature difference ΔT. The parameters are the same as those for Fig. 3.

It implies that $\lim_{t,p\to+\infty} f_t(p) = \text{const}$ and p^* may be a finite value, as has been indicated in previous studies [7].

V. GENERALIZED SSFT FOR Δs_t^m

In order to describe the process that the generalized SSFT for $p \in [0, p^*]$ approaches the conventional SSFT as t increases, we define a quantity D_t in order to quantify the time-dependent difference between the finite-time generalized SSFT and the conventional SSFT

$$D_t = \frac{1}{p^*} \int_0^{p^*} |1 - \frac{f_t(p)}{p}| \, dp, \qquad (27)$$

and one can find $\lim_{t\to+\infty} D_t = 0$ from Eq. (25).

Figure 5 shows D_t as a function of time when temperature difference ΔT varies. One can find that D_t decreases monotonically as t increases, which shows that the generalized SSFT for $p \in [0, p^*]$ monotonically approaches the conventional SSFT. Note that the greater the temperature difference, the faster the monotonic decrease of D_t. This can be understood that if the system deviates from the equilibrium state further, the medium entropy production rate, which is proportional to heat flux (see below for details), increases further. This implies stronger path irreversibility and thus the faster the generalized SSFT approaches the conventional SSFT.

Next, we investigate the anharmonic effect on the process of the generalized SSFT approaching the conventional SSFT as t increases. It can be found from Fig. 6(a) that the generalized SSFT monotonically approaches the conventional SSFT for a given anharmonic strength β. Yet D_t shows a nonmonotonic variation at a given time interval t when β increases. As shown in Fig. 6(b), one can find that the medium entropy production rate $\sigma = \frac{\langle \Delta s_t^m \rangle}{t} = (\frac{1}{T_R} - \frac{1}{T_L}) \frac{\langle q_L[X(\tau)]_t \rangle}{t}$ with $q_L[X(\tau)]_t = -\int_0^t [-\gamma v_1(\tau) + g_1 \xi_1(\tau)] v_1(\tau) \, d\tau$ gives similar nonmonotonic variation. This can be understood from the following competition mechanism of phonon transport [50]. On one hand, the increase of β enhances the scattering effect

of phonons, which inhibits the heat transport. On the other hand, the increase of β also leads to the increase of the effective phonon speed, which enhances heat transport. In terms of the fact that the effective phonon theory holds even in the regime of large anharmonic strength [50], the phonon-phonon interaction of the FPUT-β is seemingly weak from this perspective, implying quasiballistic transport is involved even in this regime [51]. When β is small, σ decreases since the phonon scattering effect dominates heat transport. When β is large, the enhancement effect play a leading role and σ increases. As mentioned above, since σ, as well as $f_t(p)$, is positively relevant with the strength of the irreversibility, the difference between the generalized SSFT and the conventional SSFT shows nonmonotonic behaviors similar to σ correspondingly.

FIG. 6. (a) D_t as a function of time interval t for different anharmonic strength β. (b) Rate of the medium entropy production $\sigma = \frac{\langle \Delta s_t^m \rangle}{t}$ as a function of β. The enlarged symbols in (b) represent σ at given anharmonic strengths β for which D_t is plotted in (a) correspondingly. Here $N = 64$ and the other parameters are the same as those for Fig. 1.
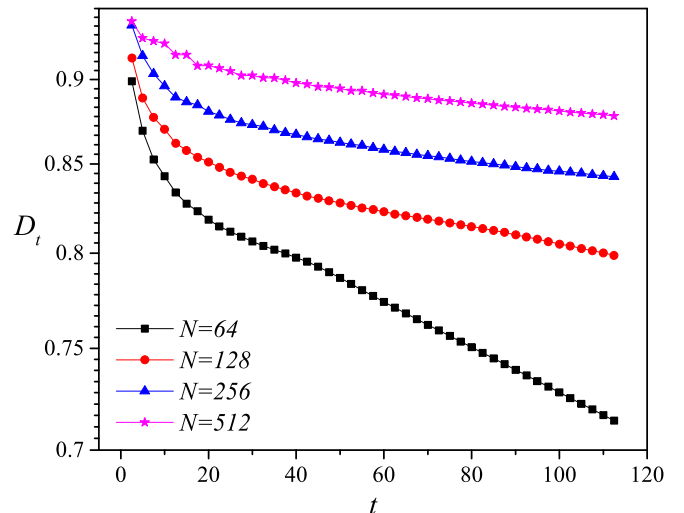
FIG. 7. D_t as a function of time interval t when the system size N varies. The other parameters are the same as those for Fig. 1.

Finally, the size effect on the time dependence of D_t is investigated. It can be found from Fig. 7 that for a given system size N, D_t tends to decrease, indicating that the generalized SSFT monotonically approaches the infinite-time conventional SSFT as t increases. Like the anharmonic strength β, since heat transport reduces when N increases, σ decreases monotonically with N, which implies the decrease of D_t.

VI. SUMMARY

In summary, we study the fluctuation of the master functional, total entropy production, and medium entropy production of one-dimensional FPUT-β chains in the nonequilibrium steady state. First, we show that for the finite-time interval t, the total entropy Δs_t^{tot} fails to satisfy the FR while the main functional R_t does, which comes from the violation of the time-reversed symmetry of the steady-state distribution for this system. Second, it is found that the medium entropy production Δs_t^m conforms to the generalized SSFT for the finite-time interval t, which generally approaches the conventional SSFT in a monotonic way regardless of the change of temperature difference, anharomonic strength, and system size. Yet the medium entropy production rate shows a nonmonotonic variation with anharomonicity, coming from the competition mechanism of phonon transport. Correspondingly, the difference between the generalized SSFT and the conventional SSFT D_t shows nonmonotonic behaviors similar to σ.

[1] D. J. Evans, E. G. D. Cohen, and G. P. Morriss, Phys. Rev. Lett. **71**, 2401 (1993).

[2] D. J. Evans and D. J. Searles, Phys. Rev. E **50**, 1645 (1994).

[3] G. Gallavotti and E. G. D. Cohen, Phys. Rev. Lett. **74**, 2694 (1995).

[4] A. Puglisi, L. Rondoni, and A. Vulpiani, J. Stat. Mech.: Theory Exp. (2006) P08010.

[5] J. Kurchan, J. Phys. A: Math. Gen. **31**, 3719 (1998).

[6] J. Lebowitz and H. Spohn, J. Stat. Phys. **95**, 333 (1999).

[7] R. van Zon and E. G. D. Cohen, Phys. Rev. Lett. **91**, 110601 (2003).

[8] G. E. Crooks, Phys. Rev. E **60**, 2721 (1999).

[9] C. Jarzynski, Phys. Rev. Lett. **78**, 2690 (1997).

[10] L. Rondoni and C. Mejía-Monasterio, Nonlinearity **20**, R1 (2007).

[11] G. Ciccotti and L. Rondoni, Aiche. J. **67**, e17082 (2021).

[12] T. M. Hoang, R. Pan, J. Ahn, J. Bang, H. T. Quan, and T. Li, Phys. Rev. Lett. **120**, 080602 (2018).

[13] U. Seifert, Phys. Rev. Lett. **95**, 040602 (2005).

[14] T. Mai and A. Dhar, Phys. Rev. E **75**, 061101 (2007).

[15] X.-G. Ma, Y. Su, P.-Y. Lai, and P. Tong, Phys. Rev. E **96**, 012601 (2017).

[16] A. Coretti, L. Rondoni, and S. Bonella, Phys. Rev. E **102**, 030101(R) (2020).

[17] A. Coretti, L. Rondoni, and S. Bonella, Entropy **23**, 146 (2021).

[18] S. Chaki and R. Chakrabarti, Physica A **511**, 302 (2018).

[19] L. Dabelow, S. Bo, and R. Eichhorn, Phys. Rev. X **9**, 021009 (2019).

[20] K. Cheng, J.-Q. Dong, W.-H. Han, F. Liu, and L. Huang, Phys. Rev. E **102**, 062127 (2020).

[21] U. Seifert, Rep. Prog. Phys. **75**, 126001 (2012).

[22] P. Visco, J. Stat. Mech.: Theory Exp. (2006) P06006.

[23] R. J. Harris, A. Rákos, and G. M. Schütz, Europhys. Lett. **75**, 227 (2006).

[24] F. Bonetto, G. Gallavotti, A. Giuliani, and F. Zamponi, J. Stat. Phys. **123**, 39 (2006).

[25] S. Lepri, R. Livi, and A. Politi, in *Thermal Transport in Low Dimensions: from Statistical Physics to Nanoscale Heat Transfer*, edited by S. Lepri, Lecture Notes in Physics, Vol. 921 (Springer, New York, 2016).

[26] H. C. Fogedby, J. Phys. A: Math. Theor. **47**, 325003 (2014).

[27] A. Kundu, S. Sabhapandit, and A. Dhar, J. Stat. Mech.: Theory Exp. (2011) P03007.

[28] A. Dhar and R. Dandekar, Physica A **418**, 49 (2015).

[29] H. C. Fogedby and A. Imparato, J. Stat. Mech.: Theory Exp. (2012) P04005.

[30] H. Touchette, Phys. Rep. **478**, 1 (2009).

[31] C. Giberti, L. Rondoni, and C. Vernia, Physica A **365**, 229 (2006).

[32] U. M. B. Marconi, A. Puglisi, L. Rondoni, and A. Vulpiani, Phys. Rep. **461**, 111 (2008).

[33] S. Lepri, R. Livi, and A. Politi, Physica D **119**, 140 (1998).

[34] T. Goldfriend and J. Kurchan, Europhys. Lett. **124**, 10002 (2018).

[35] T. Goldfriend and J. Kurchan, Phys. Rev. E **99**, 022146 (2019).

[36] A. Puglisi and D. Villamaina, Europhys. Lett. **88**, 30004 (2009).

[37] C. Maes and K. Netočný, J. Stat. Phys. **110**, 269 (2003).

[38] A. Porporato, J. R. Rigby, and E. Daly, Phys. Rev. Lett. **98**, 094101 (2007).

[39] J. M. Parrondo, C. Van den Broeck, and R. Kawai, New J. Phys. **11**, 073008 (2009).

[40] C. Van den Broeck and M. Esposito, Physica A **418**, 6 (2015).

[41] S. Denisov, S. Flach, and P. Hänggi, Phys. Rep. **538**, 77 (2014).

[42] R. C. Tolman, Phys. Rev. **23**, 693 (1924).

[43] R. C. Tolman, *The Principles of Statistical Mechanics* (Dover Publications, New York, 1979).

[44] A. Pal and S. Rahav, Phys. Rev. E **96**, 062135 (2017).

[45] D. Gupta, C. A. Plata, and A. Pal, Phys. Rev. Lett. **124**, 110608 (2020).

[46] D. Chandler, *Introduction to Modern Statistical Mechanics* (Oxford University Press, New York, 1987).

[47] S. De Groot and P. Mazur, *Non-Equilibrium Thermodynamics* (Dover Publications, New York, 2011).

[48] R. Rao and M. Esposito, Entropy **20**, 635 (2018).

[49] H. Risken, *The Fokker-Planck Equation: Methods of Solution and Applications*, 2nd ed., Springer Series in Synergetics (Springer-Verlag, New York, 1989).

[50] D. He, S. Buyukdagli, and B. Hu, Phys. Rev. E **78**, 061103 (2008).

[51] V. A. Kuzkin and A. M. Krivtsov, Phys. Rev. E **101**, 042209 (2020).